

Stability of solutions of the overdetermined inverse heat conduction problems when discretized with respect to time

Artur Maciąg

Kielce University of Technology, Kielce, Poland, and

Mohammed Jihad Al-Khatib

Ul. Piekoszowska, Kielce, Poland

Keywords Heat conduction, Inverse problems, Stability

Abstract The inverse heat conduction problem with many internal responses is considered. After discretization with respect to time, the problem is described by a system of the Helmholtz equations in a recurrent form. An approximate solution of a heat conduction problem in an integral form is shown. Then, an approximate solution of an inverse heat conduction problem in a flat slab is presented for many internal temperature responses. Stability of the solution with respect to the internal response errors is investigated for two cases: when the integrals are calculated with the use of the average value theorem and when they are calculated numerically. Analysis of the norm of a matrix that is essential for the solution stability shows that in the case of three sensors the norm slightly changes with change of the middle sensor location. If more than three sensors are taken into consideration, the results practically will not change comparing to the case of three sensors. The internal temperature response errors are suppressed if the time step is greater than a certain critical value.

Introduction

The inverse heat conduction problems (IHCPs) the paper deals with are problems of the boundary temperature identification when some thermal information at inner points of the considered body is known. They are frequently solved in an approximate way. In the paper, the first time derivative of temperature in the heat conduction equation has been replaced by the first backward finite difference. As a result, a system of the Helmholtz equations appears instead of the heat conduction equation. Such approach has been investigated in detail in Grysa (1989). In Ramesh and Lean (1991), the solution obtained in this way is compared to the analytical solution of a direct problem (i.e. an initial-boundary one) to demonstrate its effectiveness in relation to traditional methods' results. So far such an approach has been applied in case of two internal responses (IRs) when one-dimensional IHCP is considered (Grysa and Maciąg, 1998a).

The research of the first author has been supported by the National Scientific Committee in Poland, Grant No. KBN 7 T07A 033 15. The authors would like to express their gratitude to Professor K. Grysa and Professor M. Cialkowski for fruitful discussions throughout the course of this paper.

Here this approach is applied to a one-dimensional IHCP when two or more IRs are given. An IR is defined as a temperature or a heat flux measured or given at an inner point of the considered body. An internal temperature (heat flux) response will be abbreviated as ITR (IHFR). The IR at a point is known either as a continuous function or a set of discrete data. In both cases the IRs are usually inaccurate. In the paper, stability of the approximated IHCP solution is investigated with respect to the ITR errors.

The paper by Reinhardt (1993a) presents estimates for the errors of the boundary temperature or heat flux when ITRs contain a random noise. The sequential approximations for the solution of both linear and non-linear one-dimensional IHCP are analysed there. The method is then considered in Reinhardt (1993b), where the well-known method of Beck (1985) is also studied and modified.

Numerical and semi-numerical methods for solving the IHCPs, together with investigation of the errors due to ITRs inaccuracy, are presented in Kurpisz (1991) and Taler (1996). A sequential function specification technique for characterization of the boundary condition in heat treatment operations is presented in Hernandez *et al.* (1995). A problem of rapidly varying ITRs is discussed there.

Two approaches to the problem of solution stability are presented. In both, the least square method is exploited. In the first one the integrals that appear in the iterative procedure are calculated analytically. The second one is based on the spatial discretization when the integrals are calculated numerically.

The considered body is assumed to be homogeneous and isotropic with the thermal characteristics described by constant coefficients.

Discretization of the heat conduction equation with respect to time

Consider the heat conduction equation in the dimensionless form

$$\left(\nabla^2 - \frac{\partial}{\partial t}\right)T(x, t) = F(x, t) \quad , \quad (x, t) \in \Omega \times (0, \infty) \quad (1)$$

where ∇^2 denotes the Laplace operator, T stands for the relative temperature, F describes the source function, t is the dimensionless time (the Fourier number). Ω denotes the space occupied by the considered body.

The temperature T satisfies the initial condition

$$T(x, 0) = T_0(x) \quad , \quad x \in \Omega \quad (2)$$

and the boundary condition in the Dirichlet, Neumann or Robin form.

Replacing the time derivative of temperature in the equation (1) with the first backward finite difference, we arrive after some evaluation to the following system of the Helmholtz equation in a recurrent form (Grysa, 1989):

$$(\nabla^2 - p^2)T_k(x) = f_k(x) \quad , \quad x \in \Omega \quad , \quad k = 1, 2, \dots \quad (3)$$

where $T_k(x) = T(x, k\Delta t)$, $x \in \Omega$ with Δt being a dimensionless time step, $p^2 = \frac{1}{\Delta t}$ and

$$f_k(x) = -p^2 T_{k-1}(x) + p^2 \int_{(k-1)\Delta t}^{k\Delta t} F(x, t) dt, \quad k = 1, 2, \dots \quad (4)$$

The last term on the right-hand side of the formula (4) describes the mean value of the source function in the time interval $((k-1)\Delta t, k\Delta t)$.

Approximate solution of a heat conduction problem in a general case

The Helmholtz equation in m -dimensional space can be solved with the use of the potentials, described as follows:

- the single layer potential

$$S_m(x, p|h) = \int_{\partial\Omega} G_m(x - \xi, p) h(\xi) dS(\xi), \quad \xi = x_b \in \partial\Omega, \Omega \subset R^m \quad (5)$$

with h standing for a density of the potential;

- the volume potential

$$V_m(x, p|f) = - \int_{\Omega} G_m(x - y, p) f(y) dV(y), \quad x, y \in \Omega \subset R^m \quad (6)$$

with f denoting the inhomogeneity in the Helmholtz equation. $G_m(x - y, p)$ stands for the fundamental solution of the Helmholtz equation:

$$G_m(x - y, p) = \begin{cases} \frac{1}{2p} \exp(-p|x - y|) & \text{if } m = 1 \\ \frac{1}{2\pi} K_0(p|x - y|) & \text{if } m = 2 \\ \frac{1}{4\pi|x - y|} \exp(-p|x - y|) & \text{if } m = 3 \end{cases} \quad (7)$$

Here $K_0(\cdot)$ is a modified Bessel function of the second kind of the zero order.

Using the aforementioned potentials for the Helmholtz equation (3) it is possible to write its solution in an integral form. The introduced notation makes it possible to write the solution in a compact form (Grysa, 1989):

$$T_k(x) = S_m(x, p|h_k) + V_m(x, p|f_k) \quad (8)$$

In the formula (8) the single layer density h_k is an unknown function. The density $h_k (k = 1, 2, \dots)$, may be found from the temperature (or heat flux) specified on a boundary or on an inner surface for moments of time equal to $k\Delta t, k = 1, 2, \dots$. With the temperature in the form of (8) the respective integral equation for the density h_k can be then obtained with the use of a boundary condition or a prescribed internal response (ITR or IHFR) on the inner surface.

only in a sense of minimization of a certain criterion function. Let

$$J_k = \sum_{i=1}^M [T_k(x_i) - T_k^*(x_i)]^2 = \sum_{i=1}^M [f(x_i)h_k(0) + g(x_i)h_k(1) + v_k(x) - T_k^*(x_i)]^2 \quad (13)$$

describe this function. To minimize it one has to solve a system of two equations, standing for the necessary condition of the function J_k minimum, i.e.

$$\begin{cases} \frac{\partial J_k}{\partial h_k(0)} = 0 \\ \frac{\partial J_k}{\partial h_k(1)} = 0 \end{cases} \quad (14)$$

To analyze an effect of the ITRs' errors on the temperature identification error it is convenient to introduce a matrix notation. Let us denote

$$X = \begin{bmatrix} f(x_1) & g(x_1) \\ \vdots & \vdots \\ f(x_M) & g(x_M) \end{bmatrix}, T_k^* = \begin{bmatrix} T_k^*(x_1) \\ \vdots \\ T_k^*(x_M) \end{bmatrix}, V_k = \begin{bmatrix} v_k(x_1) \\ \vdots \\ v_k(x_M) \end{bmatrix}, H_k = \begin{bmatrix} h_k(0) \\ h_k(1) \end{bmatrix}, \quad (15)$$

Then, the system of equation (12) may be written down as follows

$$T_k^* = XH_k + V_k \quad (16)$$

H_k is an approximate solution of the system (16) when the function $T_k(x), 0 \leq x \leq 1$, minimizes the criterion function J_k given by the formula (13). Using the least square method we find

$$H_k = (X^T X)^{-1} X^T (T_k^* - V_k)$$

Denoting additionally

$$F(x) = \begin{bmatrix} \frac{\exp(-px)}{2p} & \frac{\exp(-p(1-x))}{2p} \end{bmatrix} = [f(x) \quad g(x)]$$

we arrive at the following form of the function describing approximately temperature $T_k(x)$ of an arbitrary point x of the slab after k time steps:

$$T_k(x) = F(x)(X^T X)^{-1} X^T (T_k^* - V_k) + v_k(x) \quad (17)$$

Stability of the approximate IHCP solution with respect to the ITRS errors

Let us examine an effect of the ITRs errors on the temperature identification error. The greatest error is expected at the boundary points that are the most distant from the IRs. As a result of investigation we are going to determine conditions concerning such location of sensors and such time steps for which the ITRs errors are not propagated in time. Let

$$\Delta_k = \begin{bmatrix} \delta T_k^*(x_1) \\ \vdots \\ \delta T_k^*(x_M) \end{bmatrix} \quad (18)$$

denote a matrix with the ITR errors in the k th step at first, second, \dots , M th internal point. We assume that all the ITR errors are of the same order.

Let $T_k^e(x)$, $T_k^d(x)$ stand for exact and disturbed temperature respectively, at a point x . The temperature identification error in the k th step at the point x may be then written as

$$\delta T_k(x) = T_k^d(x) - T_k^e(x)$$

From the formula (17) and (18) it is easy to obtain the following form of $\delta T_k(x)$:

$$\delta T_k(x) = F(x)(X^T X)^{-1} X^T (\Delta_k - (V_k^d - V_k^e)) + v_k^d(x) - v_k^e(x) \quad (19)$$

Here V_k^e , V_k^d stand for exact and disturbed values of the volume potential (comp. the formula (6)) and v_k^e , v_k^d denote exact and disturbed values of the integral in the formula (10).

The temperature identification error at the k th time step depends on the ITR errors introduced at all earlier time steps including the k th time step. It becomes evident when we notice that

$$V_k^d - V_k^e = \begin{bmatrix} \frac{\rho}{2} \int_0^1 \exp(-\rho|x_1 - y|) \delta T_{k-1}(y) dy \\ \vdots \\ \frac{\rho}{2} \int_0^1 \exp(-\rho|x_M - y|) \delta T_{k-1}(y) dy \end{bmatrix} \quad (20)$$

Without loss of generality we can confine our investigation to the point $x = 0$ (or $x = 1$), because at this point the greatest temperature error is expected. Moreover, in the IHCPs, usually the boundary temperature (heat flux) is to be found.

As it has been mentioned above we are going to determine conditions concerning such location of sensors and such time steps for which the ITRs'

errors do not propagate in time. Technically it means that the ITR error from the $(k-1)$ th time step should affect the identified boundary temperature less than the ITR error from the k th time step.

First of all, let us notice that the expression $v_k^d(x) - v_k^e(x)$ in the formula (19) may be omitted because its value (calculated with the use of the average value for integrals theorem) is negligible when compared to the term $F(x)(X^T X)^{-1} X^T (V_k^d - V_k^e)$. Then, considering the difference $\Delta_k - (V_k^d - V_k^e)$ it is enough to confine the investigation to the elements of matrix (20). With the use of the theorem on an average value for integrals we find

$$\frac{p}{2} \int_0^1 \exp(-p|x_i - y|) \delta T_{k-1}(y) dy = \delta T_{k-1}(\xi_i) \left(1 - \frac{\exp(-px_i) + \exp(-p(1-x_i))}{2} \right), \xi_i \in (0, 1) \tag{21}$$

Hence, the ITR error at the $(k-1)$ th time step affects the boundary temperature less than the ITR error introduced at the k th time step if the following inequality holds:

$$1 - \frac{\exp(-px) + \exp(-p(1-x))}{2} a, \quad \frac{1}{2}(1 - e^{-p}) \leq a \leq 1, \quad p^2 = 1/\Delta t \tag{22}$$

Note that for $a = 1$ the inequality (22) is always satisfied. It is due to the fact that x , p and $1-x$ are non-negative. It means that for $a < 1$ the ITR error from the previous time step is always suppressed in the next time step. However, the suppression rate is of great importance. Obviously, the smaller a is, the bigger suppression takes place. However, the parameter a cannot be too small. The left limit for a depends on p and x which means that the maximum suppression depends on the time step and can be achieved for $x = 0$ or $x = 1$ (see Figure 1).

Solving the inequality (22) one obtains two cases:

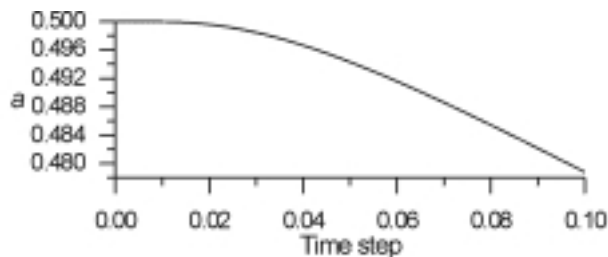


Figure 1.
The maximum suppression of an ITR error at the boundary point versus time step

(1) The inequality holds always if

$$\Delta t > \left(\frac{1}{-2 \ln(1-a)} \right)^2 \quad (23)$$

Unfortunately, the inequality (23) produces too large time steps. For example, when $a = 1/2$ then the dimensionless time step is greater than 0.5 while $a = 2/3$ leads to $\Delta t > 0.2$

(2) The inequality also holds if

$$x < \sqrt{\Delta t} \ln \frac{1-a - \sqrt{(1-a)^2 - \exp(-1/\sqrt{\Delta t})}}{\exp(-1/\sqrt{\Delta t})} \quad (24)$$

or

$$x > \sqrt{\Delta t} \ln \frac{1-a + \sqrt{(1-a)^2 - \exp(-1/\sqrt{\Delta t})}}{\exp(-1/\sqrt{\Delta t})} \quad (25)$$

Since $x \in (0, 1)$ we see that the right-hand sides of the conditions (24) and (25) describe extreme sensor location which guarantees suppression of the IR error in time. For a given value of a (being a suppression rate) the inequality (24) informs about the minimum distance from the boundary $x = 1$; the inequality (25) concerns the boundary $x = 0$.

The discussion of these two cases leads to the following conclusion:

- either the sensors are arbitrarily placed in the slab and then the time step that ensures suppression of the IR error in time can be large (which means too rough approximation of the temperature field in the slab); or
- the sensors are located near the boundary of the slab and the admissible (in the sense of the IR error suppression) time step can be small. Of course, the smaller the time step, the better approximation of the boundary temperature may be obtained.

The diagrams shown in Figure 2 illustrate the limitation of the sensor location in the slab versus dimensionless time step according to the conditions (24) and (25).

The left diagram shows that for fixed value of the suppression parameter a the points placed below the curve should be chosen as the sensor location and for fixed time step. In the right diagram the points above the curve are the proper ones. The smaller suppression parameter a is, the closer to the boundary should the sensors be placed. Concluding, we can say that in order to improve the ITR error suppression in time for a fixed time step one should

locate the ITR points (e.g. the sensors) as close to the boundary as possible. On the contrary, for a fixed time step the greater the distance from the boundary to the ITR points is, the worse results concerning the boundary temperature may be expected because of the ITR error propagation in time. And, of course, the greater the time step is, the farther from the boundary the sensors may be located.

Spatial discretization

The system of Helmholtz equation (3) describes approximately heat transfer problems when discretized with respect to time. However, the IHCPs are mostly being solved numerically. Therefore, now we are going to analyze an approximate solution of an IHCP when the problem is discretized with respect to time and space. As before, we consider an IHCP in a flat slab of a unit thickness, i.e. $x \in (0, 1)$.

Here the analysis is led for the case when the ITRs are given in an exact form.

Let x^n and x_m denote spatial discretization points ($n = 0, 1, \dots, N$) and the ITR points ($m = 1, 2, \dots, M$) respectively. We assume $N > M$. Moreover, $x^{n+1} - x^n = const$, that means the segment $(0, 1)$ is split into equal parts. In Figure 3 spatial discretization nodes as well as the ITR points are shown.

In our further consideration the formula (9) will be exploited. Because of the spatial discretization, the integral (the last expression on the right-hand side of the formula (9) denoted as $\nu_k(x)$ in formula (10)) is calculated approximately. Hence

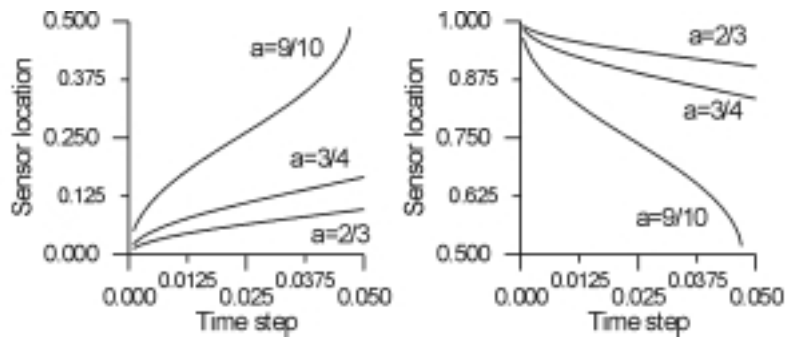


Figure 2. Sensor location versus time step for different values of the suppression parameter a . The left diagram illustrates the condition (24), the right one – the condition (25)

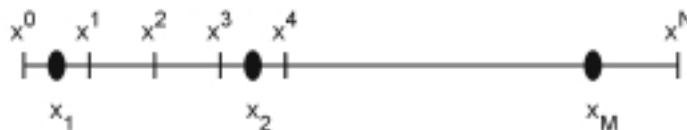


Figure 3. Nodes of the segment $(0, 1)$ division and ITR points location

$$\begin{aligned}
 v_k(x_m) &= \frac{p}{2} \int_0^1 \exp(-p|x_m - y|) T_{k-1}(y) dy = \\
 &= \frac{p}{2N} \left(\frac{1}{2} e^{-p|x_m - x^0|} T_{k-1}(x^0) + e^{-p|x_m - x^1|} T_{k-1}(x^1) \right. \\
 &\quad \left. + \dots + e^{-p|x_m - x^{N-1}|} T_{k-1}(x^{N-1}) + \frac{1}{2} e^{-p|x_m - x^N|} T_{k-1}(x^N) \right) \quad (26)
 \end{aligned}$$

Let

$$T_k = \begin{bmatrix} T_k(x^0) \\ \vdots \\ T_k(x^N) \end{bmatrix}_{(N+1) \times 1}$$

stand for a temperature distribution at the division nodes of the slab in the k th moment of time. Additionally, denoting

$$E^* = \frac{p}{2N} \begin{bmatrix} \frac{1}{2} e^{-p|x_1 - x^0|} & e^{-p|x_1 - x^1|} & \dots & e^{-p|x_1 - x^{N-1}|} & \frac{1}{2} e^{-p|x_1 - x^N|} \\ \vdots & \vdots & & \vdots & \vdots \\ \frac{1}{2} e^{-p|x_M - x^0|} & e^{-p|x_M - x^1|} & \dots & e^{-p|x_M - x^{N-1}|} & \frac{1}{2} e^{-p|x_M - x^N|} \end{bmatrix}_{M \times (N+1)} \quad (27)$$

by virtue of (15), (10) and (26) we obtain

$$V_k^* = E^* T_{k-1} \quad (28)$$

The stars in the formulas (27) and (28) are due to the ITR point coordinates that appear there.

Let us introduce a matrix E (analogous to E^*) as follows:

$$E = \frac{p}{2N} \begin{bmatrix} \frac{1}{2} e^{-p|x^0 - x^0|} & e^{-p|x^0 - x^1|} & \dots & e^{-p|x^0 - x^{N-1}|} & \frac{1}{2} e^{-p|x^0 - x^N|} \\ \vdots & \vdots & & \vdots & \vdots \\ \frac{1}{2} e^{-p|x^N - x^0|} & e^{-p|x^N - x^1|} & \dots & e^{-p|x^N - x^{N-1}|} & \frac{1}{2} e^{-p|x^N - x^N|} \end{bmatrix}_{(N+1) \times (N+1)}$$

Denoting additionally

$$F = \frac{1}{2p} \begin{bmatrix} e^{-px^0} & e^{-p(1-x^0)} \\ \vdots & \vdots \\ e^{-px^N} & e^{-p(1-x^N)} \end{bmatrix}_{(N+1) \times 2}$$

we arrive at the following formula describing a temperature of any point of the slab at the k th moment of time:

$$T_k = F(X^T X)^{-1} X^T (T_k^* - E^* T_{k-1}) + E T_{k-1} \tag{29}$$

or

$$T_k = A T_k^* + B T_{k-1} \tag{30}$$

where $A = F(X^T X)^{-1} X^T$ and $B = E - F(X^T X)^{-1} X^T E^*$. The matrix B decides on convergence of the iterative process described by the formula (30).

Define a matrix norm as follows (Demidowicz and Maron, 1965):

$$\|B\| = \sqrt{\lambda_{\max}(B^* \cdot B)}$$

where $\lambda_{\max}(B^* \cdot B)$ denotes the greatest eigenvalue of the matrix $B^* \cdot B$. B and B^* stands for the matrix conjugate to the matrix B .

The process is convergent if the norm of the matrix B is less than 1 (Demidowicz and Maron, 1965).

For three ITRs ($M = 3$) left and right diagrams presented in Figure 4 show the dependence of the matrix B norm on the third and first ITR point location respectively, for the dimensionless time step equal to 0.005, when the second ITR point is placed at $x_2 = 0.5$. The first diagram is drawn for $x_1 = 0.1$; the second one – for $x_3 = 0.9$.

The diagrams in Figure 4 show that the norm of matrix B depends mostly on location of the sensor being more distant from the closest boundary point. Hence, we can assume $x_3 = 1 - x_1$.

The diagrams presented in Figure 4 have been obtained for $N = 300$. Of course, increasing the number of nodes in the segment $\langle 0, 1 \rangle$ division leads to better accuracy in the integral calculation. The matrix B norm values obtained

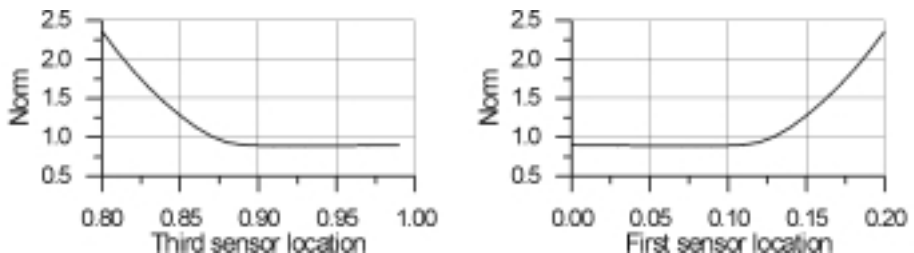


Figure 4.
Matrix B norm versus
the sensor location

for $N = 300$ and for $N = 600$ and for different third sensor location are shown in Table I. A greater number of the node points causes practically no changes of the matrix B norm when $\|B\| < 1$ and slightly changes its value otherwise (comp. the left diagram in Figure 4).

Figure 5 illustrates the matrix B norm dependence on the middle sensor location in the case of $M = 3$ (i.e. for three ITRs) for $x_1 = 0.01$, $x_3 = 0.99$ and $\Delta t = 0.005$.

The diagram is symmetric with respect to $x = 0.5$, because $x_3 = 1 - x_1$. Figure 5 shows that for $M = 3$ the matrix B norm practically does not depend on the location of the middle sensor. Dependence of the matrix B norm on the dimensionless time step for $x_1 = 0.01$, $x_2 = 0.5$, $x_3 = 0.99$ is shown in Figure 6 when the segment is split into 300 parts ($N = 300$).

Figure 6 shows that in the case $M = 3$ for too small time steps the iterative process (30) may be divergent. This conclusion can be extended for $M > 3$. It is shown in Figure 7, done for $M = 4$.

Analysis of Figure 7 leads to the following conclusion: the fourth IR point practically does not change the matrix B norm. Considering the set of the IR points we see that the number of sensors being placed between the two located outside with respect to the others has no significant influence on the matrix B norm. Hence, solving the one-dimensional IHCP in a flat slab it is enough to use three sensors to obtain internal responses. More sensors do not improve results significantly and, what is obvious from the physical point of view, they rather disturb the temperature field than help in obtaining better results.

The diagram in Figure 8 illustrates the dependence of the matrix B norm on the first and second sensor location in the case when $M = 3$, $x_3 = 1 - x_1$, $x_1 < 0.5$, $x_1 < x_2 < x_3$, $\Delta t = 0.005$.

Again (compare conclusions following Figure 5) we note that the matrix B norm depends mainly on x_1 and x_3 , i.e. on the extreme sensors location.

x_3	0.8	0.82	0.84	0.86	0.88	0.9	0.92	0.94	0.96	0.98	1.0
$N = 300$	2.36	1.85	1.45	1.13	0.93	0.89	0.89	0.89	0.89	0.90	0.90
$N = 600$	2.34	1.84	1.43	1.11	0.93	0.89	0.89	0.89	0.89	0.90	0.90

Table I. Values of the matrix B norm obtained for $N = 300$ and for $N = 600$ and for different third sensor location

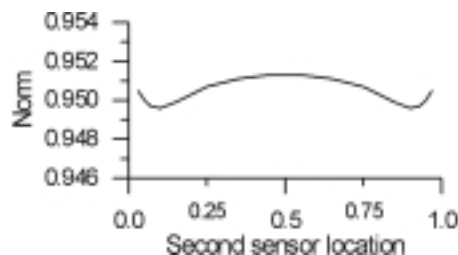


Figure 5. Matrix B norm versus second sensor location

The matrix B norm becomes greater than 1 when the time step is too small (compare Figure 6) or when the two sensors located outside with respect to the others are located too far from the boundary (compare Figure 4 and Figure 8). Therefore, the following question has to be answered: what means “too far” in the case of fixed time step, if the matrix B norm is to be smaller than 1? The answer is presented in Figure 9.

In order to have $\|B\| < 1$ the points placed below the curve in Figure 9 should be chosen as the sensor location for a given time step. It is worth noting that for the time step greater than circa 0.088 the matrix B norm is smaller than 1 independently of the location of sensors. On the other hand, if the time step is smaller than circa 0.00035 then the matrix B norm is greater than 1 for any location of sensors.

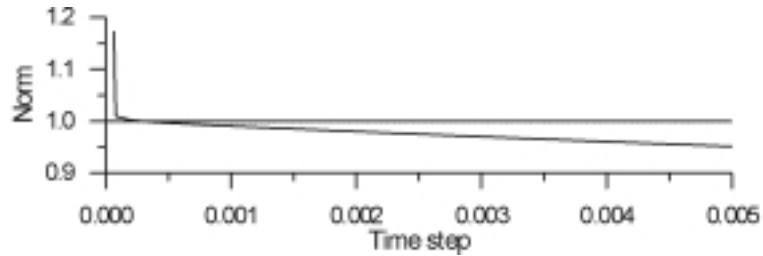


Figure 6.
Matrix B norm versus time step length

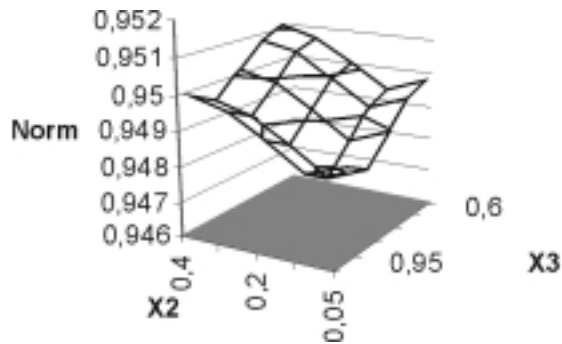


Figure 7.
Matrix B norm versus x_2 and x_3 for $x_1 = 0.01$, $x_4 = 1 - x_1 = 0.99$ and $\Delta t = 0.005$

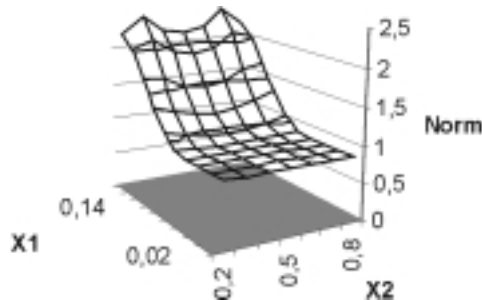


Figure 8.
Matrix B norm versus x_1 and x_2 for $\Delta t = 0.005$

The main conclusion resulting from the above analysis (when the ITRs are given in exact form) is that only if the time step is greater than a certain limit value depending on the sensor location then the iterative process (30) is convergent.

Analysis of the ITR error propagation with the use of the spectral norms of the introduced matrices

Assume an ITR in the k th time step is given with a certain error. Let δT_k^* stand for the matrix of the aforementioned errors. Then, by virtue of (30),

$$T_k = AT_k^{*e} + A\delta T_k^* + BAT_{k-1}^{*e} + BA\delta T_{k-1}^* + B^2T_{k-2} \quad (31)$$

where the superscript e denotes the exact temperature. Let

$$\nu = \frac{\|(BA)^T(BA)\|}{\|A^T A\|}$$

denote quotient of the spectral norms of the matrices BA and A . Stability of the iterative process described by the formula (30) will be ensured if the ITR error from the $(k-1)$ th time step will affect the field of temperature calculated in k th step less than the ITR error from the k th time. It means that an inequality $\nu - 1$ has to be satisfied. Moreover, the term B^2T_{k-2} should be negligible.

By virtue of the analysis from the previous section we can confine our consideration to the case $M = 3$. We also assume $x_3 = 1 - x_1$ and $x_2 = 0.5$. In Figure 10 a dependence of the quotient ν on the time step is presented for $x_1 = 0.01, x_2 = 0.5, x_3 = 0.99$ and $N = 600$. Of course, we concentrate on the case $\nu < 1$.

From Figure 10 it is clear that the ITR error is suppressed if the dimensionless time step is greater than a certain critical value. In the case of $x_1 = 0.01, x_2 = 0.5, x_3 = 0.99$ when the quotient ν is of the order 0.3 then the term B^2T_{k-2} becomes negligible. From Figure 10 one can note that the dimensionless time step is then of the order 0.0001.

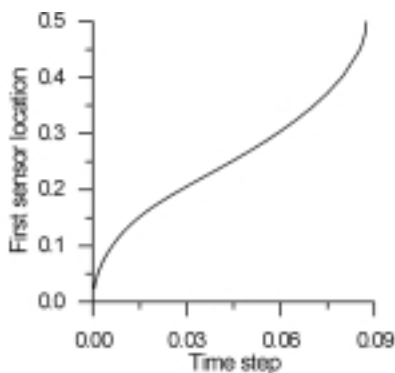


Figure 9.
The first sensor location versus time step when $\|B\| = 1; x_2 = 0.5, x_3 = 1 - x_1$

In Figure 11 a dependence of ν on the first sensor location (i.e. the point x_1) is shown. Here $\Delta t = 0.001$, $x_3 = 1 - x_1$, $x_2 = 0.5$ and $N = 600$. Of course, we are interested in values of ν less than 1.

Figure 11 confirms the earlier conclusion that in the case of three ITRs for better ITR error suppression in time the outer (first and third) sensors should be placed close to the boundary of the flat slab (i.e. close to $x = 0$ or $x = 1$ respectively).

The next diagram, presented in Figure 12, shows a dependence of the quotient (on the dimensionless time step and on the first sensor location for $x_3 = 1 - x_1$ and $x_2 = 0.5$. We can note that to have $\nu = 1$ in the case of small time steps the first sensor should be placed close to the boundary $x = 1$ (e.g. for $\Delta t = 0.02$ we find x_1 of the order 0.1). To have $\nu < 0.3$ for $\Delta t = 0.02$ the value of x_1 should be of the order 0.05.

Figure 10.
The quotient ν versus the dimensionless time step

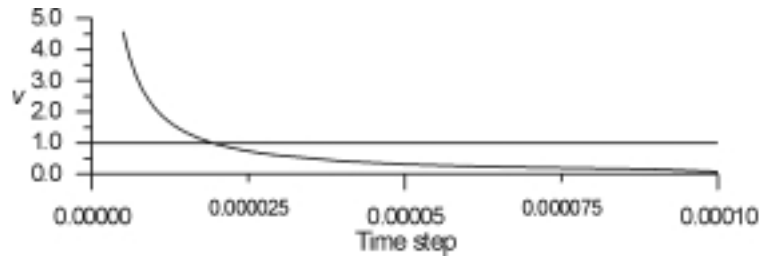


Figure 11.
The quotient ν versus the first ITR point location

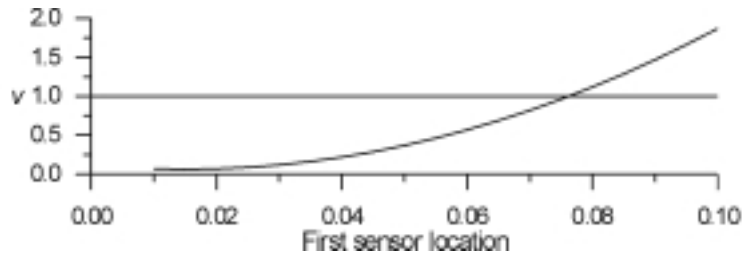
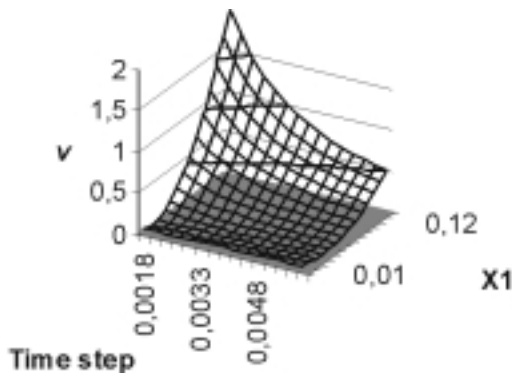


Figure 12.
The quotient ν versus the dimensionless time step and the first sensor location



The last diagram, in Figure 13, shows the dependence of the first sensor location, x_1 , on such a dimensionless time step for which the quotient ν is equal to 1 (solid line). Then, the ITR error is not suppressed and it is not amplified either. In order to have the ITR error suppressed for a fixed time step one has to locate the first sensor at a point indicated by the area below the solid line. The asterisk line illustrates the upper limit for the point x_1 location found from the formula (24) with the suppression parameter $a = 19/20$.

Comparing both the solid and the asterisk lines, one can find a remarkable agreement between the results obtained with two different methods.

Conclusions

The accurate determination of the heat transfer boundary condition is a crucial component of mathematical models aimed at predicting the evolution of the thermal, microstructural and stress fields in heat treatment operations, e.g. Taler (1996; 1997); Hernandez *et al.* (1995). Therefore, a question of the IHCP solution stability is one of the most important in the theory of the ill-posed problems. Here that question has been discussed for the one-dimensional IHCP.

The conclusions derived from this work can be summarized as follows:

- (1) The ITR error does not propagate in time in two cases:
 - either the sensors are arbitrarily placed in the slab and then the time step that ensures suppression of the IR error in time can be large (that means too rough approximation of the temperature field in the slab); or
 - the sensors are located near the boundary of the slab and the admissible (in the sense of the IR error suppression) time step can be small. Of course, the smaller time step is, the better approximation of the boundary temperature may be obtained.
- (2) Analysis of an effect of the inner sensors (placed between the two located outside with respect to the others) on the approximate solution stability is practically the same for three and for more than three

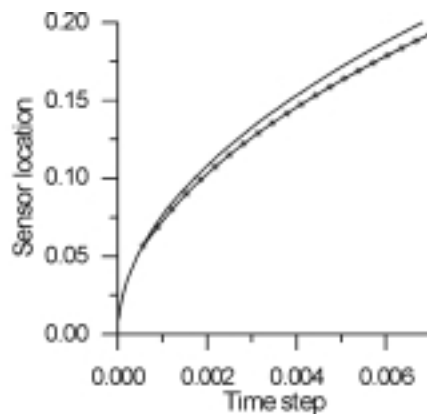


Figure 13. The first sensor location versus the time step for which the quotient ν is equal to 1 (s line) and versus the upper limit for the point x_1 location found from the formula (24) for $a = 19/20$ (asterisk line)

sensors. It means that when dealing with an IHCP in a slab it is enough to use three sensors in order to record the ITRs.

In many cases a shape of a two- and three-dimensional body may be approximately described as a flat slab or cylindrical or spherical layer. Consider an element of the body with known internal responses that can be approximately described as a flat slab. Then, using dimensionless coordinates the characteristic data concerning the IHCP in a flat slab have to be determined. Finally, using one of the diagrams presented in the paper, the time step that ensures stable calculations can be found.

In the case of cylindrical and spherical layers, an analysis similar to the one presented in this paper may be done. Diagrams concerning the stability conditions for these cases will be presented in Grysa and Maciąg (in preparation).

References

- Beck, J.V., Blackwell, B., St. Clair Jr, Ch.R.St. (1985), *Inverse Heat Conduction – Ill-posed Problems*, Wiley-Interscience, New York, NY, Chichester, Brisbane, Toronto, Singapore.
- Demidowicz, B.P. and Maron, I.A. (1965), *Numerical Methods*, PWN, Warszawa (in Polish).
- Grysa, K. (1989), "On the exact and approximate methods of solving the inverse problems of temperature fields", *Rozprawy, Politechnika Poznańska*, 204, Poznań (in Polish).
- Grysa, K. and Maciąg, A. (1998a), "Stability investigation for the inverse heat conduction problems", *Advanced Computational Method in Heat Transfer V*, Computational Mechanics Publications, Southampton, and Boston, MA, pp. 93-102.
- Grysa, K. and Maciąg, A. (1998b), "On stability of some overdetermined inverse heat conduction problems", *Advanced Computational Method in Heat Transfer V*, Computational Mechanics Publications, Southampton and Boston, MA, pp. 415-24.
- Grysa, K. and Maciąg, A., "Stability of solutions of the inverse heat conduction problems for the bodies of cylindrical and spherical shape" (in preparation).
- Hernandez-Morales, B., Brimacombe, J.K. and Hawbolt, E.B. (1995), "Characterization of the boundary condition in heat treatment operations using an inverse heat conduction algorithm", *ASME Heat Transfer Division (Publication) HTD*, ASME, New York, NY, pp. 559-66.
- Kurpisz, K. (1991), "Numerical solution of one case of inverse heat conduction problems", *Journal of Heat Transfer, Trans. ASME*, Vol. 113 No. 2, pp. 280-6.
- Ramesh, P.S. and Lean, M.H. (1991), "Accurate integration of singular kernels in boundary integral formulations for Helmholtz equation", *International Journal for Numerical Methods in Engineering*, Vol. 31 No. 6, pp. 1055-68.
- Reinhardt, H.-J. (1993a), "Towards a stability and error analysis of sequential methods for the inverse heat conduction problem", *Proc. 1 Int. Conf. Inverse Probl. Eng. Theory Pract. Publ by ASME*, New York, NY, pp. 11-16.
- Reinhardt, H.-J. (1993b), "Analysis of sequential methods of solving the inverse heat conduction problem", *Numerical Heat Transfer, Part B: Fundamentals*, Vol. 24 No. 4, pp. 455-74.
- Taler, J. (1996), "Semi-numerical method for solving inverse heat conduction problems", *Heat and Mass Transfer/Waerme- und Stoffuebertragung*, Vol. 31 No. 3, pp. 105-11.
- Taler, J. (1997), "Analytical solution of the overdetermined inverse heat conduction problem with an application to monitoring thermal stresses", *Heat and Mass Transfer/Waerme- und Stoffuebertragung*, Vol. 33 No. 3, pp. 209-18.